

Thermodynamic Assessment of the Fe–Mn Binary Alloy System using the CALPHAD Method

D.F. Khan¹, W.U. Khan¹, W.U. Shah^{1*}, H.U. Shah¹, H.Q. Yin²,
A.G.Mamalis³

¹*Department of Physics, University of Science and Technology, Bannu 28100, Khyber Pakhtunkhwa, Pakistan*

²*School of Materials Science and Engineering, University of Science and Technology, 100083 Beijing, P.R. China*

³*Project Centre for Nanotechnology and Advanced Engineering (PC-NAE), NCSR–Demokritos, Athens, Greece*

Email: waseemullahshah303@gmail.com

Thermodynamic assessment of and predictions for the metastable binary iron–manganese alloy (Fe–Mn system) have been undertaken using the CALPHAD (calculation of phase diagram) method. Phase diagrams, Gibbs energies of mixing, excess Gibbs energies, thermodynamic molar activities, coefficient of activities, and partial and integral values of enthalpy have been calculated at three elevated temperatures: 1200, 1225 and 1250 K. The alloy shows positive deviations from Vegard’s and Henry’s laws (the latter deviation being small) and corresponding negative deviation from Raoult’s law (ideal Gibbs curve). Results show that the ferromagnetic state of the Fe–Mn alloy is the most stable. Phase equilibria show almost ideal characteristic behaviour. Overall the alloy is at equilibrium and has good stability.

Keywords: PBIN database, phase diagram.

1. Introduction

Mn is a very well reported element for the evolution of significant magnetic steels such as TWIP steels, which have good strength and ductility. Lattice stability of Mn and Fe was first investigated using the CALPHAD method by Schwerdtfeger and S. Bigdeli [1-2]. The method has been used for the developing and modeling thermodynamic properties of many materials for four decades. A complete CALPHAD-based assessment of Fe–Mn system was carried out by A.T. Dinsdale and W.Huang. [3-4]. The thermochemical approach for the Fe–Mn system was formulated by B.J. Lee et al [5]. The martensitic-like transformation for

Fe-based alloys regarding the sigma phase (fcc-A1) and Gibbs energy optimization was studied in refs [6] and [7]. Eutectoid-based reactions for the Fe–Mn alloy system appear to be relatively insignificant. Magnetism plays a major role in the stabilization of the gamma phase at the lower eutectoid temperature. The activity of Mn in the alloy was assessed using CALPHAD [8-9].

The present research into the Fe–Mn system uses the third generation of the Thermo-Calc software package and CALPHAD database. The optimization of the Fe–Mn system and the Fe–Mn–Si system transformation enthalpy was assessed.

2. Results and Discussion

2.1 Phase diagram

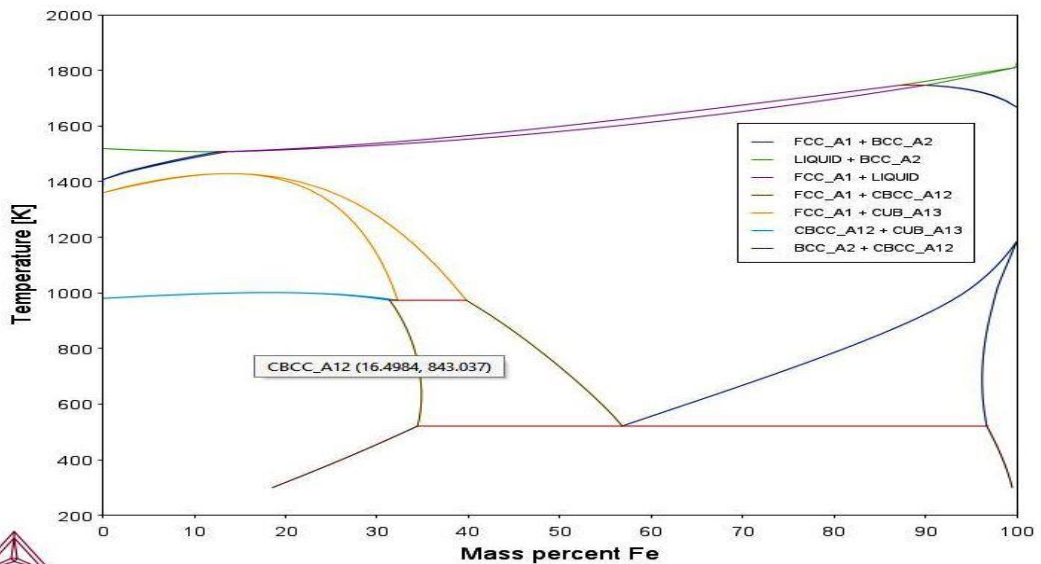


Figure 1. Computed phase diagram of the Fe-Mn alloy, shows face centred cubic, liquid, cumulative base centered cubic. the abscissa gives x_{Mn} , the fraction of Mn atoms in the alloy. Fig. 1 shows the phase diagram of the ferric-manganese binary alloy system by the applications of Calphad method with Thermo-Calc package. different natured solid and liquid phases have investigated by applying temperature range (1200-1250K). (10-90) mass percent of Fe results the highest stability phase FCC with austenite coordinations. CBCC phase with 16.4984 mass% of the Mn results the corresponding stability in connection to BCC regim with ferrite coordination. the alloy seems less metastable range for whole range compositions. Results are in good agreement with available experimental results and previous assessments by E.J. Mittemeijer [10]. The phase transformation FCC-A1 (austenite), BCC-A2 (ferrite phase), and FCC-A1/HCP-A3 (martensitic) of the phase diagram calculated by researchers in the Fe-Mn system with all solution phases as liquid, BCC-A12, BCC-A2, CUB-A13, FCC-A1, CPH-A3, CPH-A3 phases and shows metastable one accordance as the phases have calculated by Redlich-kister polynomial calculations. Mn as a transition metal plays a vital role in the creation of magnetic properties for the said alloy system. The CPH-A3 phase being metastable creates homogenous heterogeneity in the phase structure of the system and makes variational based characteristics for the solid solution. Previous research results show that the ferromagnetic state of Mn-Fe-C alloy is the most stable. Investigated results report

many magnetic-based moments of atoms [11]. For Mn and Fe system, their measured phase equilibria show activity curve data for solid in almost ideal behavior, but somehow small positive deviation from ideality. Stable phase diagram for the Fe-Mn system has been investigated in accordance with A. Christou, D.D. Johnson, and D. Birnie's recommendations [12-14]. The ferromagnetic phase is the most stable phase in that particular alloy system with occurring at the ground state. As a transition metal alloys the magnetic properties if the said alloy is very complex natured depends on the alternation of thermal energy and curie temperatures. The magnetism is responsible for creating stable nature properties in that alloy system with low-temperature ranges [15]

$$G^q = x_{Fe}^0 G_{Fe}^q + x_{Mn}^0 G_{Mn}^q + G_m^q + G_{mag}^q \quad (1)$$

Where G is the Gibbs free energy of a system is for pure element, for Mn, Fe, Gibbs energy paramagnetic state value is 298.15k. , while the other parameters x, G^m molar fraction, molar Gibbs energy, and magnetic-based ordering of the system,

$$G_m^q = RT[x_{Fe} \ln x_{Fe} + x_{Mn} \ln x_{Mn}] + G^{qs} \quad (2)$$

While R is gas constant with excess molar Gibbs energy. Here the Redlich-Kister power series is used for mathematical manipulations as

$$G_N^{q,s} = x_{Fe} x_{Mn} \sum_{v=0}^n L^q_{Fe, Mn} (x_{Fe} - x_{Mn})^v \quad (3)$$

Now by Calphad convention rule

$${}^vL^q_{Fe, Mn} = a_v^q + b_v^q T + c_v^q T \ln T + d_v^q T^2 + e_v^q T^3 + f_v^q T^{-1} + g_v^q T^7 + h_v^q T^{-9} \quad (4)$$

With “a” and “h” are the imperial parameters. ^vL^q is the angular momentum term for v-q state. While a_v^q, b_v^q, c_v^q, d_v^q, e_v^q, f_v^q, g_v^q, h_v^q are the activities of the a-h states in magnetic orbital transition of the particular alloy system. x_{Fe}, x_{Mn} shows the composition range for both alloys.

Here the bcc-A2 of ferromagnetic phase shows magnetic contribution to this particular system, bcc-A12, cph-A3, fcc-A1, while cph-A3 shows anti ferromagnetic contributions to this system, as in accordance with A.T. Dinsdale calculations [16]

$$G_{mag}^q = RT \ln (B^q + 1) \quad (5)$$

While for numerical solution, if g (t) < 1 then we will observe as

$$g(t) = 1 - (79t^{-1}/140 p + 474/497(1/p - 1) (t^3/6 + t^9/135 + t^{15}/600))/D \quad (6)$$

$$G(t) = - (t^{-5}/10 + t^{-15}/315 + t^{-25}/1500)/D \quad \text{if } t > 1 \quad (7)$$

$$\text{While } D = 0.46044 + 0.73189(1/(p - 1)) \quad (8)$$

t = T/T_{C,N} that represents a particular curie temperature of **q-Th** phase during transformation from ferromagnetic to paramagnetic transformation, similarly anti ferromagnetic to paramagnetic. **G_{mag}^q**, shows the magnetic part of gibbs energy of orbitals. RT shows the enternal energy corrwsponding to entropy of the system. information about average magnetic moment, as well the crystal structure of that particular alloy system [17], the value of **P** is 0.40 for bcc-A2, while for fcc-A1, BCC-A12, CPH-A3 are 0.38. so

$$C_{pmag}^q = RT \ln (Bq + 1) \quad (9)$$

$$C(t) = 474/497(1/p - 1) (2r^3 + 2t^9/3 + 2t^{15}/5) \quad (10)$$

$$D, \quad \text{if } t < 1 \quad C(t) = (2t^{-5} + 2t^{-15}/3 + 2t^{-25}/5)/D \quad \text{if } t > 1 \quad (11)$$

The proposed prediction in the Fe-Mn alloy system shows contribution to the ferromagnetic and anti-ferromagnetic phases and their transformation as in accordance with literature through Calphad method.

3. Thermodynamic modeling

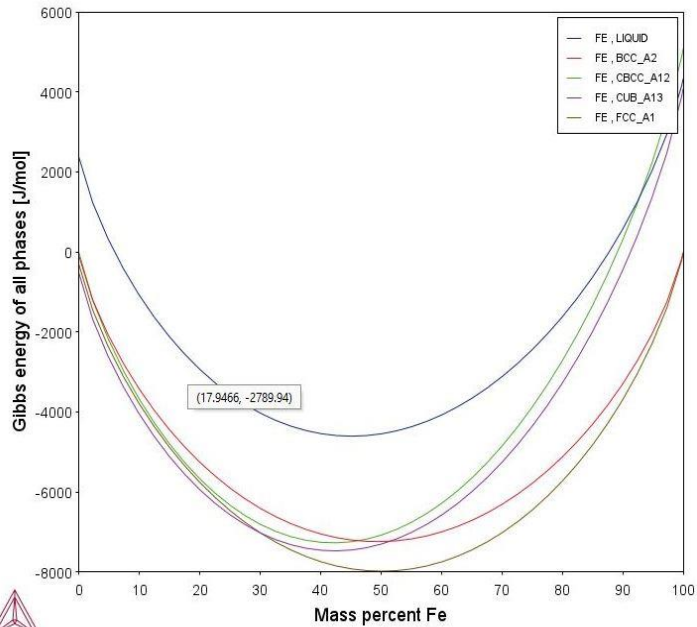


Fig:2 (a) shows gibbs free energy of Fe-Mn at 1250K (GMR). The atmospheric pressure applied 10^6 pascal for simulations

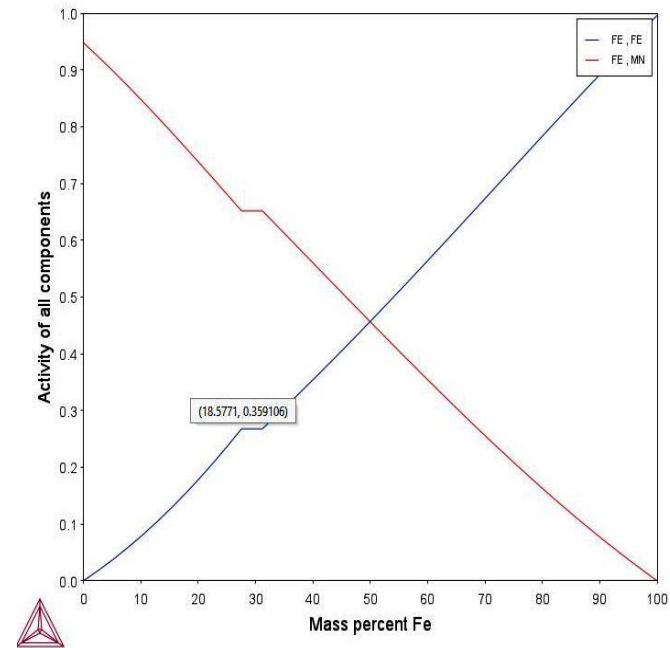


Fig:2 (b) shows Activity Fe-Mn at 1225K the thermodynamic activity vs mass fraction of stable phases is given.

Fig.2 a,b , shows corresponding curves for Gibbs free Energy and thermodynamic molar Activity of the Fe-Mn alloys system at different elevated temperature ranges (1200-1250)K respectively. The Gibbs energy curves versus different temperature show that the only phase survives at the last is FCC-A1, the negativity of this phase shows Raoult’s law accordance and more stability of the Fe-Mn alloy system at this particular alloying stage. The fluctuations of other phases are also important for heterogeneity; at 1250k the most stable phase is ferrite characteristics. the proceeding table 1 showing for showing the results of the simulations in the Fe-Mn system.

The results are precise and based on database discriptions.the gibbs energy ,activity of phases vs temperature profile is assessed.

Table, 1: DATABASE THERMODYNAMIC phase CALCULATION AT TEMPERATURE: 1200K, 1225K, 1250K for the system: Fe-Mn

T°:K	Press ure:pa scal	Number of moles	ACRX (activity of a component relative ratio (Mn)	Mass:gr am	Total Gibbs energy:j/ mol	Volum e :cm3	Enthalp y:j/mol	Activit y Fe. SER:st able element referen ce state	Activity Mn. SER: stable element reference state
1200K	1.000 00*10 ⁵	1.0000	100000*10 ⁻²	5.58378 *10 ¹	- 5.72895* 10 ⁴	7.2277 2*10 ⁻⁶	3.5020 2*10 ⁴	9.8984 8*10 ⁻¹	1.01648*10 ⁻²
--	--	--	--	--	--	--	--	9.9000 8*10 ⁻¹	1.00008*10 ⁻²
--	--	--	--	--	--	--	--	3.3925 8*10 ⁻³	1.4088*10 ⁻⁵
--	--	--	--	--	--	--	--	- 5.6733 8*10 ⁴	-1.1145*10 ⁵
FCC_A 1#1	--	1.00000	--	5.5838* 10 ¹	--	--	--	--	--
--	--	--	--	--	--	--	--	9.9000 0*10 ⁻¹	1.00000*10 ⁻²
1225K	--	1.00000	1*10 ⁻²	5.58378 *10 ¹	- 5.92215* 10 ⁴	7.2409 4*10 ⁻⁶	3.5876 2*10 ⁴	9.8984 *10 ⁻¹	1.0164*10 ⁻²
--	--	--	--	--	--	--	--	9.9000 *10 ⁻¹	1.0000*10 ⁻²
--	--	--	--	--	--	--	--	3.1547 *10 ⁻³	1.3321*10 ⁻⁵
--	--	--	--	--	--	--	--	- 5.8656 *10 ⁴	-1.1434*10 ⁵
FCC_A 1#1	--	1.000	--	5.5838* 10 ¹	--	--	--	9.9000 0*10 ⁻¹	1.00000*10 ⁻²
1250K	1.000 008*1	1.0000	--	5.58378 *10 ¹	- 6.11710* 10 ⁴	7.2541 8*10 ⁻⁶	3.6737 5*10 ⁴	9.8984 *10 ⁻¹	1.0164*10 ⁻²

	0 ⁵				10 ⁴				
--	--	--	--	--	--	--	--	9.9000 *10 ⁻¹	1.0000*10 ⁻²
--	--	--	--	--	--	--	--	2.9372 *10 ⁻³	1.2600*10 ⁻⁵
--	--	--	--	--	--	--	--	- 6.0595 *10 ⁴	-1.1725*10 ⁵
FCC_A 1#1	--	1.0000	--	5.5838* 10 ¹	--	--	--	9.9000 0*10 ⁻¹	1.000008*10 ⁻²

Table 1: Shows thermodynamic fluctuations and results of Fe-Mn during alloying at temperature of 1200K, the Gibbs energy of the alloying acquires a value of -5.72895×10^4 J/mol. The Enthalpy of the system reach a value of 3.50202×10^4 J/mol corresponding to Gibbs energy. The molar activity of Fe and Mn is fluctuating a values (9.8984×10^{-1} , 9.90000×10^{-1} , 3.3925×10^{-3} , -5.6733×10^4 , 9.9000×10^{-1} , $(1.0164 \times 10^{-2}$, 1.0000×10^{-2} , 1.4088×10^{-5} , 1.00000×10^{-2} , -1.1145×10^5) while the surviving phase here is FCC-A1#1 with high stability. Increasing the temperature upto 1225K, the Gibbs energy becomes -5.92215×10^4 J/mol with further decreasing its value, while enthalpy acquire a more positive value of 3.58762×10^4 J/mol. The molar activity fluctuation at these temperature is for Fe, Mn element as (9.8984×10^{-1} , 9.9000×10^{-1} , 9.90000×10^{-1} , -5.8656×10^4 , 3.1547×10^{-3}), (1.0164×10^{-2} , 1.0000×10^{-2} , 1.00000×10^{-2} , -1.1434×10^5 , 1.3321×10^{-5}) with FCC-A1#1 phase as a stable phase for the given temperature. At 1250K of last temperature interval in our study the Total Gibbs energy reaches its highest negative value of -6.11710×10^4 J/mol and highest positive value of enthalpy 3.67375×10^4 J/mol. Which shows that the system is going toward most stability even if the repulsive interaction is more active. The thermodynamic molar Activity of Fe, Mn elements are highest fluctuation as (9.8984×10^{-1} , 9.9000×10^{-1} , 2.9372×10^{-3} , 9.90000×10^{-1} , -6.0595×10^4), (1.0164×10^{-2} , 1.0000×10^{-2} , 1.00000×10^{-2} , -1.1725×10^5 , 1.2600×10^{-5}) with highest stable phase in the phase diagram FCC-A1#1. The activity of Fe is maximum as (9.90000×10^{-1}) while smaller for Mn elements. The system shows non equilibrium and stable state at highest given temperature. The Fe-Mn system is more reliable in stability and industrial needs.

4. Conclusion

The thermodynamic analysis is shown using Calphad method with pbin database of thermo-calc package, all thermodynamic optimization is of fluctuating nature, and shows compositional heterogeneity, no equilibrium is found in the said alloy system and shows metastable nature accordance. With the increasing temperature in Fe-Mn binary alloy system, the enthalpy of the system increases gradually by existing repulsion forces among alloying elements which show positive deviation from Vegard's law, and found accordance with previous results, but the alloy still shows stability by decreasing their Gibbs energy value regularly with increasing enthalpy, which shows negative deviation from Raoult's law. The total Gibbs energy of the Fe-Mn system decreases with increasing temperature, which shows the stability of Fe-Mn system. The peak negative deviation is observed at 1250 K which shows a strong negative deviation in the Fe-Mn system and increasing the stability level means enhancing the hardness, wear resistance, corrosion resistance, and another

doping characteristic of the said alloy. Ferromagnetic (FM) state of Mn-Fe alloy is the most stable one phase and occupied at the ground state. For Mn and Fe system, the measured phase equilibria show activity curve data for solid in almost ideal behavior, but somehow small positive deviation from ideality is observed. A stable phase diagram for the Fe-Mn system has been investigated in accordance with Hallowell's recommendations. The FM phase is most stable phase in that particular alloy system with occurring at the ground state. As a transition metal alloys, the magnetic properties of the Fe-Mn alloy system are very complex natured and depends on the alternation of thermal energy and curie temperatures. This favors the lower temperature. The magnetism is responsible for creating stable nature properties in that alloy system with low temperature ranges.

The enthalpy proportion with temperature shows the increase in the heat contents of the said alloy system and we observed maximum enthalpy at 1250K, which is responsible for the withstanding and surviving high temperature and high heat-absorbing capacity of Fe-Mn alloy system, activity shows throughout fluctuation from Vegard's law in a positive sense, which shows the system complex nature with rare doping and shows his greater validity for industrial variety in the system of interests and research areas.

References

1. S. Bigdeli, H. Mao Och, M. Selleby, On the third generation Calphad databases, an updated description of Mn. *physica status solidi b*. 252 (2015) 2199-2208.
2. K. Schwerdtfeger, Measurement of oxygen activity in iron, iron–silicon, manganese, and iron–manganese melts using solid electrolyte galvanic cells. *Trans. Met. Soc. AIME* . 239 (1967) 1276-1281.
3. A.T. Dinsdale, SGTE data for pure elements. *Calphad*. 15 (1991) 317–425.
4. W. Huang, An assessment of the Fe–Mn system. *Calphad*. 13 (1989) 243-252.
5. B.J. Lee, D.N. Lee, A thermodynamic study on the Mn–C and Fe–Mn systems. *Calphad*. 13 (1989) 345-354.
6. J. Martinez, S.M. Cotes, J. Desimoni, Enthalpy change of the hcp/fcc martensitic transformation in the Fe–Mn and Fe–Mn–Si systems. *J. Alloys Compounds*. 479 (2009) 204–209.
7. J. Nakano, P. Jacques, Effects of the thermodynamic parameters of the hcp phase on the stacking fault energy calculations in the Fe–Mn and Fe–Mn–C systems. *Calphad*. 34 (2010) 167–175.
8. V.T. Witusiewicz, F. Sommer, E.J. Mittemeijer, Reevaluation of the Fe–Mn phase diagram. *J. Phase Equilibria Diffusion*. 25 (2004) 346–354.
9. R. Kubitz, F.H. Hayes, Enthalpies of mixing in the iron–manganese system by direct reaction Calorimetry. *Mh. Chem.* (1987) 31–41.
- 10 F. Damay, J. Sottmann, F. Lainé, L. Chaix, M. Poienar, P. Beran, E. Elkaim, F. Fauth, L. Nataf, A. Guesdon, A. Maignan, and C. Martin, Magnetic phase diagram for Fe_{3–x}MnxBO₅. *Phys. Rev. B* 101(2020) 094418.
11. Dejan Djurovic, Richard Dronskowski, thermodynamic assessment of Fe-Mn-c system. *Calphad*. 35(2011)479-491.
12. D.D. Johnson, F.J. Pinski, G.M. Stocks, Effects of chemical and magnetic disorder in Fe_{0.50}Mn_{0.50}. *J. Appl. Phys.* 63 (1988) 3490.
13. D. Birnie, E.S. Machlin, L. Kaufman, K. Taylor, Comparison of pair potential and thermochemical models of the heat of formation of BCC and FCC alloys. *Calphad*. 6 (1982) 93-
Nanotechnology Perceptions Vol. 19 No.2 (2023)

126.

14. A. Christou High-Pressure Phase Transition and Demagnetization in Shock Compressed Fe[Single Bond]Mn Alloys. *Journal of Applied Physics*. 42,11(1971) 4160 – 4170.
- 15 T. Gebhardt, D. Music, B. Hallstedt, M. Ekholm, I.A. Abrikosov, L. Vitos, J.M. Schneider, Ab initio lattice stability of fcc and hcp Fe–Mn random alloys, *Journal of Phys: Condens. Matter*, 22 (2010) 295-402.
16. A.T. Dinsdale: “Scientific Group Thermo-data Europe Database for Pure Elements,” *Calphad journal*. 15(1991) 317-425.
17. Zhenxin Li, Yang Zhang et al, Research Progress of Fe-Based Superelastic Alloys, *Crystals* 12,5 (2022) 602